Physiological and Pathological Rhythms:
Role of Feedback in Stability and Periodicity

A Project Report

submitted by

CELESTINE PREETHAM (EE09B010)

in partial fulfilment of the requirements
for the award of the degree of

BACHELOR OF TECHNOLOGY

DEPARTMENT OF ELECTRICAL ENGINEERING
INDIAN INSTITUTE OF TECHNOLOGY MADRAS.

MAY 2013

THESIS CERTIFICATE

This is to certify that the thesis titled **Physiological and Pathological Rhythms: Role of Feedback in Stability and Periodicity**, submitted by **Celestine Preetham (EE09B010)**, to the Indian Institute of Technology, Madras, for the award of the degree of **Bachelor of Technology**, is a bona fide record of the research work done by him under my supervision. The contents of this thesis, in full or in parts, have not been submitted to any other Institute or University for the award of any degree or diploma.

Prof. Gaurav Raina
Research Guide
Professor
Dept. of Electrical Engineering
IIT-Madras, 600 036

Place: Chennai

Date: May 14, 2013

ACKNOWLEDGEMENTS

I express my heartfelt thanks to my mentor Dr. Gaurav Raina. He has been instrumental in making me realize the importance, challenges, and, joy behind good academic writing. Apart from academics, through my research work, he has inspired into me valuable life lessons, such as paying attention to detail and effective communication.

ABSTRACT

KEYWORDS: Physiological control system; Delay differential equation; Mackey-Glass equation; Lasota equation; Local stability analysis; Local bifurcation analysis; Hopf bifurcation.

We study a class of physiological systems which are modeled by nonlinear delay differential equations. In particular, we focus on the Mackey-Glass and Lasota equations which have been proposed to model the erythrocyte concentration in blood. These equations are prototypical of several other physiological systems and hence are interesting in a broader context.

For both these systems, we conduct a systematic local stability, local rate of convergence and local Hopf bifurcation analysis. We show that the system behaves like a damped oscillator in the stable regime and obtain expressions for critical damping. After a critical delay, the system loses stability and is proved to undergo a Hopf bifurcation. The system is reduced to a two dimensional center manifold and then transformed to the Hopf bifurcation normal form. Limit cycle amplitudes are computed analytically and corroborated through bifurcation simulations.

The study and control of oscillatory instabilities and chaos provides insights for effective treatment strategies of certain dynamical diseases like cardiac arrhythmia and Parkinson tremors. Closed form expressions for critical damping, critical delay and amplitude of limit cycles enable us to design controllers for these systems.

Contents

List of Tables

List of Figures

ABBREVIATIONS

$x(t)$	State variable (concentration of erythrocyte in blood)
x_*	Equilibrium point
$p(\cdot)$	Production function
$d(\cdot)$	Destruction function
β	Production coefficient
γ	Destruction coefficient
n	Exponent factor
τ	Feedback time delay
$W[\cdot]$	Lambert W-function

$\lambda + a + b\exp(-\lambda\tau) = 0$ is the first order characteristic equation

λ_i	$\lambda_i = \sigma_i + \mathrm{j}\omega_i$ are the set of solutions to the characteristic equation
ROC	Rate of Convergence $\equiv Min(-\sigma_i)$
τ_c	Critical delay $= {}^{\arccos(a/-b)}/_{\sqrt{b^2-a^2}}$
Θ	Degree of stability $= \arccos\left(\frac{a}{-b}\right)$

$\sqrt{\mu/\mu_2}$	Amplitude of limit cycles for Hopf bifurcation at $\tau = \tau_c + \mu$

Chapter 1

Introduction

1.1 Motivation

Physiological processes like heartbeat and breathing have been observed to be rhythmic (periodic) (Glass and Mackey, 1988) under normal conditions, but can switch to new rhythms or chaotic behavior under special conditions like physical exertion or the onset of a disease. Mackey and Glass (1977) proposed that, the oscillatory instabilities correspond to a bifurcation in the dynamics of an underlying first order delay differential equation. Such changes is qualitative dynamics based on parameter variations is called a *dynamical disease.* See Bélair *et al.* (1995); Mackey and Milton (1987) for a review of dynamical diseases that arise in hematology, cardiology, neurology, and psychiatry. A class of physiological systems can be modeled by the nonlinear delay differential equation (an der Heiden and Mackey, 1982)

$$\dot{x}(t) = p\left(x\left(t-\tau\right)\right) - d\left(x\left(t\right)\right), \tag{1.1}$$

‘

where $p\left(\cdot\right)$ is a production function, $d\left(\cdot\right)$ is a destruction function and τ is a feedback delay. For several physiological systems, the destruction function is linear (an der Heiden and Mackey, 1982) and given by

$$d\left(x\right) = -\gamma x, \tag{1.2}$$

where γ is the rate constant.

In particular, we study the Mackey and Glass (1977) and Lasota (1977) equations that have been proposed to model the erythrocyte concentration in blood. These equations are prototypical of several other mixed feedback systems.

an der Heiden and Mackey (1982) proved that a mixed feedback system has stable

and unstable limit cycles, where the cycles may have an arbitrary number of extrema per period. They proved period doubling and chaos for a rectangular feedback function. In this paper, we numerically simulate the same for some smooth feedback functions. We explain the appearance of limit cycles through a Hopf bifurcation analysis.

See Bélair *et al.* (1995) for a review on the identification, temporal aspects and treatment strategies of human illness based on modeling it as a dynamical disease. For example, a cardiac arrhythmia suppression trial (Echt *et al.*, 1991) found an increase in sudden cardiac deaths in patients receiving a drug that reduced certain types of cardiac arrythmia. In the presence of chaos, even small changes in drug concentration can change a potential beneficial effect to an effect that causes significant patient morbidity or even mortality. To that end, the study and control of chaotic dynamics is achieved by a robust system design. A simple approach is to choose operating parameters that are far from the Hopf bifurcation manifold. Beuter and Vasilakos (1995) demonstrated bistability between a large amplitude Parkinson tremor and a physiological tremor. This can be understood as due to a subcritical Hopf bifurcation. Hence, stability and bifurcation analysis is useful in the diagnosis, therapy, and device design for such diseases.

1.2 Organization

In Chapter 2, we introduce two nonlinear time-delayed models (Mackey-Glass and Lasota) and show that they satisfy physiological constraints like boundedness and positivity. We numerically simulate the Mackey-Glass equation and present graphs to illustrate the influence of time delay on the system dynamics. In Chapter 3, we linearize the system about the fixed points and list conditions for local stability using results obtained in Appendix A. We then analyze the effect of model parameters on the rate of convergence of the linearized systems. We show that the system behaves like a damped oscillator and obtain expressions for critical damping. The expressions for stability and rate of convergence are illustrated in stability charts. In Appendix B, we prove that the system undergoes a Hopf bifurcation on losing local stability and calculate the amplitude of the resulting limit cycles. In Chapter 4, we present a Hopf bifurcation diagram that corroborates our estimate for limit cycle amplitudes. Finally, in Chapter 5, we present our inferences and list out avenues for further research.

Chapter 2

Nonlinear time-delayed models

Figure 2.1 shows a control system for the concentration of erythrocytes in blood, $x\,(t)$. Such a control system can be modeled by

1. *Mackey-Glass equation* (Mackey and Glass, 1977) :

$$\dot{x\,(t)} = \beta\frac{x(t-\tau)}{1+x(t-\tau)^n} - \gamma x(t) \tag{2.1}$$

2. *Lasota equation* (Lasota, 1977) :

$$\dot{x\,(t)} = \beta x\,(t-\tau)^{\,n} \exp\left(-x\,(t-\tau)\right) - \gamma x\,(t) \tag{2.2}$$

where $\beta > 0$ is the production coefficient, $\gamma > 0$ is the destruction coefficient, $\tau > 0$ is a time delay, and $n > 0$ is an exponent.

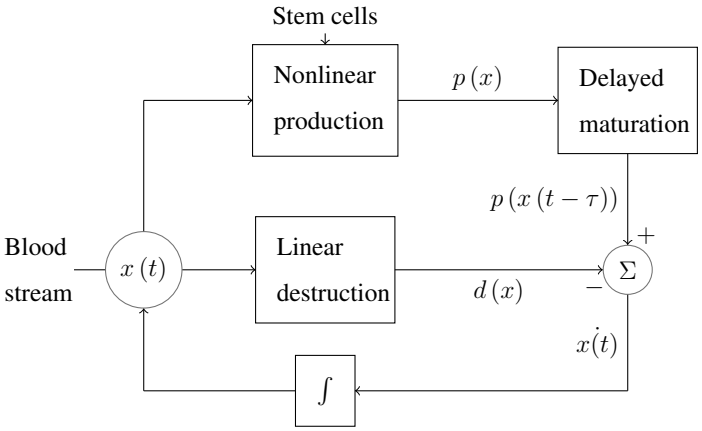

Figure 2.1: Erythrocyte life cycle in human blood (Mackey, 1997). Stem cells and erythrocytes interact to produce cells that mature into erythrocytes. The average time to mature corresponds to a feedback delay τ in the production chain. Erythrocytes are assumed to be destroyed at a rate constant γ.

2.1 Positivity and boundedness

It is useful to obtain bounds on $x\,(t)$ based on its past dynamics. We prove boundedness for (1.1) if the production function $p\,(\cdot)$ is positive and bounded by the destruction function $d\,(\cdot)$. Note that (2.1) and (2.2) satisfy these conditions.

Lemma 1. *If $x(t)$ is positive for $t < t'$, and if $p(x) > 0\ \forall x > 0$; then $x(t)$ remains positive $\forall t < t' + \tau$.*

Proof. $\dot{x}(t) = p(x(t-\tau)) - \gamma x(t)$

$\implies \dot{x}(t) > -\gamma x(t)$

$\implies x(t) > x(t') \exp(-\gamma(t-t')) > 0.$ □

Theorem 2. *If $x(t)$ is positive for $t < t'$, and if $p(x) > 0\ \forall x > 0$; then $x(t)$ remains positive $\forall t$.*

Proof. By induction on Lemma 1. □

Corollary 3. *If $x(t)$ is bounded above by $\bar{x}$ for $t < t'$, and if $p(x) < d(\overline{x})\ \forall x < \bar{x}$; then $x(t)$ remains bounded above $\forall t$.*

Proof. $x(t) \leftarrow \overline{x} - y(t)$ in (1.1) and (1.2) yields $\dot{y}(t) = (d(\overline{x}) - p(x(t-\tau))) - \gamma y(t)$.

$y(t)$ is positive by Theorem 2 and hence $x(t)$ is bounded above by $\bar{x}$. □

Corollary 4. *If $x(t)$ is bounded below by $\bar{x}$ for $t < t'$, and if $p(x) > d(\overline{x})\ \forall x > \bar{x}$; then $x(t)$ remains bounded below $\forall t$.*

Proof. Consider $x(t) \leftarrow \overline{x} + y(t)$ in (1.1) and (1.2). □

2.2 Qualitative system dynamics

Bounded systems can either converge to an equilibrium point, a limit cycle, or a chaotic attractor. Figure 2.2 illustrates the dependence of the system dynamics on the delay τ for the Mackey-Glass equation. The delay τ destabilizes the system into limit cycles and then to chaotic oscillations. However, an optimum delay τ_0 can result in faster convergence of the linearized system.

In Figure 2.3, we see that, apart from a trivial equilibrium point- there can exist either a unique stable equilibrium point, a saddle-node, or a pair of stable and unstable equilibrium points. Throughout this paper, we only consider the stable equilibrium point.

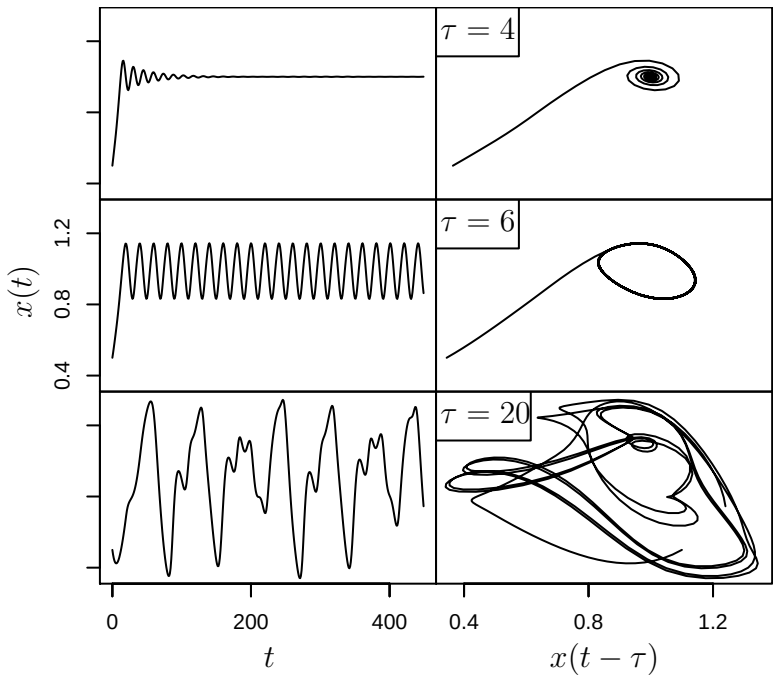

Figure 2.2: The system described by the Mackey-Glass equation (2.1), on increasing the delay τ; transitions from equilibrium point convergence, to limit cycles, and to chaotic oscillations. Simulated using MATHEMATICA (Wolfram Research, 2010), with $\gamma = 0.1$, $\beta = 0.2$, $n = 10$ and $x(t) = 0.5 + 0.02t$, $-\tau \leq t < 0$.

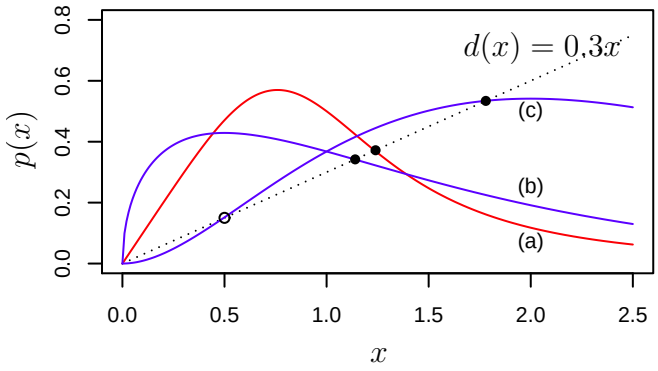

Figure 2.3: The above figure plots different production functions $p(x)$ and shows, at $\tau = 0$, the local stability of non-zero equilibrium points obtained for $d(x) = 0.3x$. The equilibrium point is unstable when $p'(x) > d'(x)$ as shown in Section A. Expressions for non-zero equilibrium points and conditions for their existence are given in Table 3.1. The Mackey-Glass equation can only have a unique stable equilibrium point. The Lasota equation can have either a unique stable equilibrium point, a saddle-node, or a pair of stable and unstable equilibrium points. *(a)* Mackey-Glass equation (2.1) with $\beta = 1, n = 4$. *(b)* Lasota equation (2.2) with $\beta = 1, n = 0.5$. Whenever $n < 1$, it has a unique stable equilibrium point. *(c)* Lasota equation with $\beta = 1, n = 2$. Whenever $n > 1$, for $\gamma/\beta < \left(^{n-1}/_{\mathrm{e}}\right)^{n-1}$, it has two equilibrium points given by the Lambert W-function. The smaller equilibrium point is unstable and hence we only consider the larger equilibrium point. At $\gamma/\beta = \left(^{n-1}/_{\mathrm{e}}\right)^{n-1}$, it undergoes a saddle-node bifurcation.

Chapter 3

Linearization

Linearizing (1.1) about the stable equilibrium point x_* , and letting $x\left(t\right) = x_* + y\left(t\right)$, we have

$$\dot{y\left(t\right)} = -ay(t) - by(t-\tau), \tag{3.1}$$

where x_*, a and b are listed in Table 3.1. We can obtain the necessary and sufficient conditions for stability by carrying out the local stability analysis as in Section A. We present our results in Table 3.1.

Table 3.1: Linearization about the equilibrium point.

	Mackey-Glass equation (2.1)	**Lasota equation (2.2)**
Condition for equilibrium	$\frac{\gamma}{\beta} < 1$	$\frac{\gamma}{\beta} < \left(\frac{n-1}{\mathrm{e}}\right)^{n-1}$ or $n < 1$
x_*[a]	$\left(\frac{\beta-\gamma}{\gamma}\right)^{\frac{1}{n}}$	$(1-n)W\left[(\gamma/\beta)^{\frac{1}{n-1}}/(1-n)\right]$
a	γ	γ
b	$\gamma\left(n\left(1-\frac{\gamma}{\beta}\right)-1\right)$	$\gamma\left(x_*-n\right)$
Unconditional stability	$1 > \frac{\gamma}{\beta} > \frac{n-2}{n}$	$\left(\frac{n-1}{e}\right)^{n-1} > \frac{\gamma}{\beta} > \left(\frac{n+1}{e}\right)^{n-1} e^{-2}$
Sufficient condition	$\tau\gamma\left(n\left(1-\frac{\gamma}{\beta}\right)-1\right) < \frac{\pi}{2}$	$\tau\gamma\left((n+1)\log\left[\frac{\beta}{\gamma}\left(\frac{n+1}{e}\right)^{n-1}\right]\right) < \pi$

[a] $W\left[\cdot\right]$ is the Lambert W-function.

3.1 Rate of convergence

The linearized physiological models in Table 3.1 have a first order transcendental characteristic equation

$$\lambda + a + b\exp(-\lambda\tau) = 0. \tag{3.2}$$

Let $\lambda_i = \sigma_i + \mathrm{j}\omega_i$ be the set of solutions to the characteristic equation (3.2). Then we define the rate of convergence (ROC) as

$$ROC \equiv Min\left(-\sigma_i\right).$$

Theorem 5. *ROC is maximum when the system is critically damped. This happens at $\tau_0 = \frac{W\left[\frac{a}{eb}\right]}{a}$.*

Proof. Consider the characteristic equation (3.2)

$$\implies (\lambda\tau + a\tau)\exp\left(\lambda\tau + a\tau\right) + b\tau\exp\left(a\tau\right) = 0$$

$$\implies \lambda\tau + a\tau = W\left[-b\tau\exp\left(a\tau\right)\right]$$

$$\implies \lambda = a\left(-1 + \frac{W[-b\tau\exp(a\tau)]}{a\tau}\right).$$

We also have,

$$\frac{d\lambda}{d\tau} = \frac{-(\lambda + a)\lambda}{\tau(\lambda + a) + 1} = \frac{-(\lambda + a)\lambda}{1 + W\left[-b\tau\exp\left(a\tau\right)\right]}.$$

For $W\left[-b\tau_0\exp\left(a\tau_0\right)\right] = -1$, $\frac{d\lambda}{d\tau}$ is singular. Hence λ has a local extrema at $\tau_0 = \frac{W\left[\frac{a}{eb}\right]}{a}$.

$$ROC \equiv \Re\left[-\lambda\right] = a - \frac{\Re\left[W\left[-b\tau\exp\left(a\tau\right)\right]\right]}{\tau}.$$

As $\frac{-d\lambda}{d\tau} > 0$ for $\tau < \tau_0$, the ROC has a maxima at τ_0.

λ is complex for $\tau > \tau_0$ and real for $\tau \leq \tau_0$. Hence, the system is critically damped at τ_0.

$$ROC_{max} = a\left(1 + W\left[\frac{a}{eb}\right]^{-1}\right).$$

□

We can see from Figure 2.2 that the system spirals into asymptotic stability. We consider the distance of $(x(t), x(t-\tau))$ from the equilibrium point as an indicator of convergence. Figure 3.1 corroborates our claim.

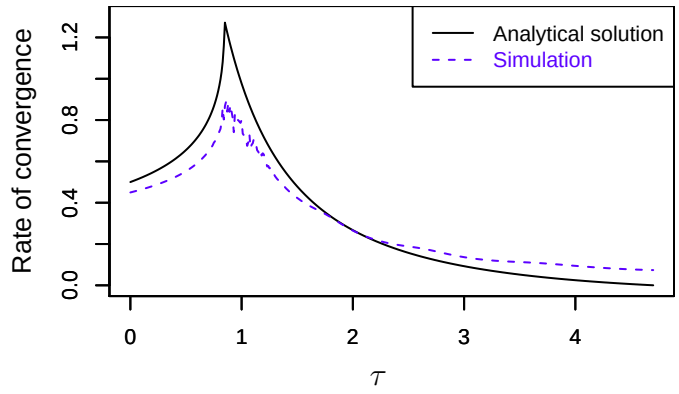

Figure 3.1: We compare the numerically simulated ROC against the analytical solution. The numerical ROC is obtained by taking the logarithmic distance of $(x(t), x(t-\tau))$ from the equilibrium point, at $t = 30$. The analytical solution is computed by linearizing the system. The system can be understood as a damped oscillator with the feedback delay τ acting as a damping factor. We have simulated using MATHEMATICA (2010), taking $\gamma = 0.1$, $\beta = 0.2$, $n = 10$ and $x(t) = 0.5 + 0.02t$, $-\tau \leq t < 0$.

In Figure 3.2, we have numerically computed the stability characteristics of the Lasota equation and visually represented the Hopf bifurcation lines and rate of convergence.

3.2 Local stability charts

In Figure 3.3, we present local stability charts. Note that it suffices to plot representative regions of local stability in the $\beta-\gamma$ and $\tau-n$ planes to capture the change in qualitative dynamics along any parameter variation.

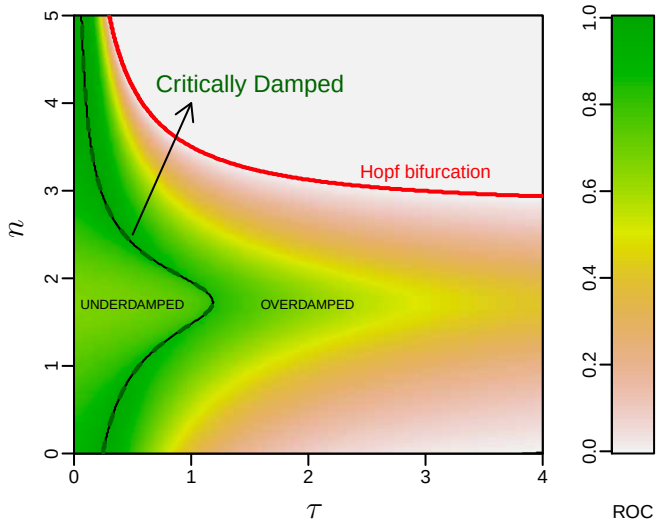

Figure 3.2: In this gradient plot, we characterize the convergence of the linearized Lasota equation (2.2) along the $\tau - n$ plane at $\beta = 4, \gamma = 1$. The critically damped line (ROC_{max}) signifies the transition between underdamped (non-oscillatory) and overdamped (oscillatory) convergence. The system loses convergence as it approaches the Hopf bifurcation manifold.

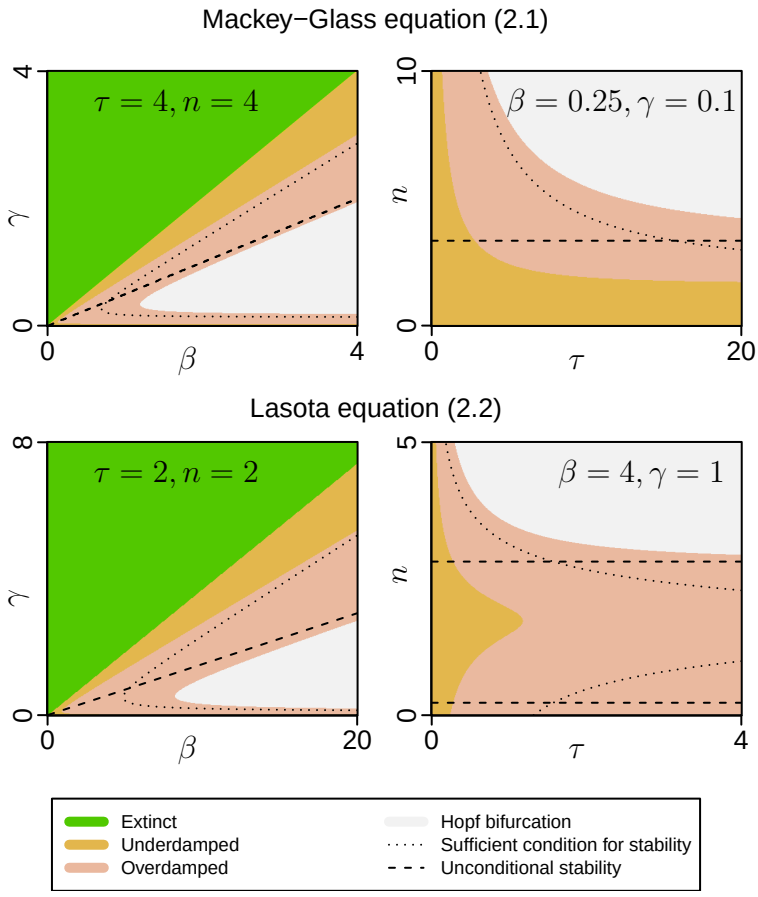

Figure 3.3: Local stability charts. These charts illustrate the system's sensitivity to parameter variations. We shall show that the system undergoes a Hopf bifurcation at loss of stability. For a robust system, it is desirable to be far from the Hopf bifurcation line and close to critical damping.

Chapter 4

Hopf bifurcation

We have shown in the Appendix that the physiological systems undergo Hopf bifurcations. In order to compare the bifurcation dynamics of different models, we set them on a common platform. The parameters of the different models may be chosen such that they are equivalent under linearization. We choose $\gamma = 1$ for both models and choose other parameters (β, n) such that they give the same equilibrium point x_* and critical delay τ_c. We take τ as the common bifurcation parameter to perform the analysis in B and present our result in Figure 4.1.

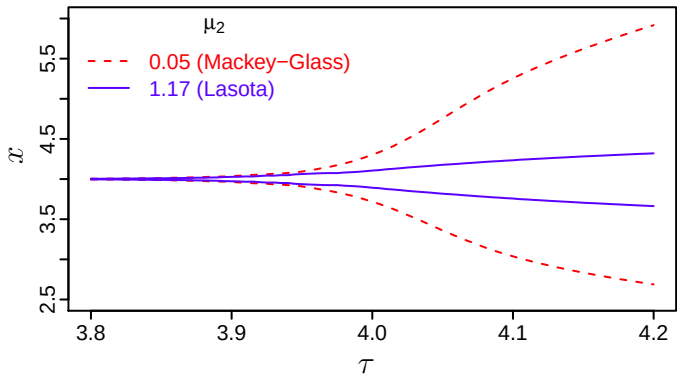

(a) $x_* = 4, \tau_c = 4$.

Figure 4.1: We contrast the bifurcation dynamics for the Mackey-Glass (2.1) and Lasota (2.2) equations. The amplitude of the limit cycles (Appendix B) is proportional to $\sqrt{1/\mu_2}$. This is corroborated by the above numerical simulations.

Chapter 5

Conclusion

We have performed a systematic study of the nonlinear delay differential equation (1.1) which is prototypical of several physiological systems. In particular, we studied equations (2.1) and (2.2) that model erythrocyte concentration in human blood. We proved boundedness and positivity of the system if the production function is bounded by the destruction function. We performed a local stability analysis and presented conditions for stability in Table 3.1.

In the asymptotically stable regime, the system is observed to behave like a damped oscillator transitioning from non-oscillatory to oscillatory convergence. In Theorem 5, we have shown that the rate of convergence is maximum at critical damping. Figure 3.1 validated numerical simulations against the analytical solution for rate of convergence of the linearized system. Figure 3.2 showed the existence of a critical damping manifold. It is of interest to operate at critical damping for robust treatment of dynamical diseases. We presented local stability charts (Figure 3.3) that aid in the design of robust systems.

Further, we did a local bifurcation analysis and calculated the amplitude of limit cycles. In Figure 4.1, we illustrate bifurcation diagrams that corroborate our analysis. We obtained analytic expressions for the Lyapunov coefficient. In this paper, we have only performed a local stability and local bifurcation analysis. It is important to research and develop a similar systematic procedure for global stability and global bifurcation analysis.

Appendix A

Local stability analysis for transcendental characteristic equations

The linearized physiological systems in Section 3.1 have a first order transcendental characteristic equation

$$\lambda + a + b\exp(-\lambda\tau) = 0. \tag{A.1}$$

λ_k is the k^{th} eigenvalue satisfying (A.1). For asymptotic stability, $\Re(\lambda_k) < 0 \; \forall \, k$. Hence, asymptotic stability at $\tau = 0$ requires $b > -a$. On increasing τ, λ_k move from the left half plane towards the right half plane. Let τ_c be the smallest delay for which $\exists k$ such that $\Re(\lambda_k) = 0$. Putting $\lambda_k = \mathrm{j}\omega_0$ in (A.1) yields

$$\begin{aligned} \omega_0 - b\sin(\omega_0\tau_c) &= 0, \\ a + b\cos(\omega_0\tau_c) &= 0. \end{aligned}$$

Solving for ω_0, we get $\omega_0^2 + a^2 - b^2 = 0$. We have,

1. No positive solution for ω_0^2 if $|b| \leq a$. The system is unconditionally stable.
2. Unique positive solution for ω_0^2 if $b > a$ and $a > 0$. We get the critical delay

$$\tau_c = \frac{\arccos\left(\frac{a}{-b}\right)}{\sqrt{b^2 - a^2}}. \tag{A.2}$$

It is useful to introduce a parameter

$$\Theta = \arccos\left(\frac{a}{-b}\right)$$

that captures the degree of stability. We have $\frac{\pi}{2} < \Theta < \pi$ and $b\tau_c = {}^{\Theta}/_{\sin\Theta}$. It is easy to see that $\tau_c > \frac{\pi}{2b}$. Hence $\tau < \frac{\pi}{2b}$ is a sufficient condition for stability when $b > a > 0$. As $\Theta \to \pi^-$, $\tau_c \to \infty$ and becomes unconditionally stable. As $\Theta \to \frac{\pi}{2}^+$, $\tau_c \to \frac{\pi}{2b}$ and can be seen as a maximally unstable system.

Appendix B

Local bifurcation analysis

In order for a Hopf bifurcation to occur at $\tau = \tau_c$, we first need to satisfy the *transversality condition* (Kuznetsov, 1998), i.e.

$$\Re\left(\frac{d}{d\tau}\lambda_k\right)\Bigg|_{\tau=\tau_c} \neq 0.$$

On differentiating (A.1), we get

$$\frac{d}{d\tau}\lambda_k\Bigg|_{\tau=\tau_c} = \frac{-(\lambda+a)\lambda_c}{\tau_c(\lambda_c+a)+1},$$

We obtain

$$\alpha'(0) \equiv \Re\left(\frac{d}{d\tau}\lambda_k\right)\Bigg|_{\tau=\tau_c} = \frac{\tau_c(b^2-a^2)}{1+2a\tau_c+b^2\tau_c^2} > 0$$

since $b > a > 0$ for existence of τ_c. The transversality condition is thus always satisfied. A Hopf bifurcation occurs whenever the *nondegeneracy condition* (nonzero Lyapunov coefficient) is also satisfied (Kuznetsov, 1998).

B.1 Center manifold reduction to the Hopf bifurcation complex normal form

Let $\tau = \tau_c + \mu$ with a Hopf bifurcation taking place at $\mu = 0$. The system needs to be reduced to a two dimensional Hopf bifurcation complex normal form

$$\dot{w} = \left(\frac{\mu}{\mu_2} + \mathrm{i}\right) w + w\left|w\right|^2 + O\left(\left|w\right|^4\right). \tag{B.1}$$

In order to characterize the local stability of limit cycles generated at Hopf bifurcation point, it is sufficient to approximate the nonlinearity by considering only the quadratic and cubic terms. The amplitude of limit cycles can be shown to be $\sqrt{\mu/\mu_2}$ for small μ (Kuznetsov, 1998).

All other characteristic roots at τ_c except $\pm \mathrm{j}\omega$ have negative real parts. According to the center manifold theorem (Carr, 2006), there is a family of smooth two-dimensional invariant manifolds W_μ^c near the origin. The infinite dimensional system restricted on W_μ^c is two-dimensional and has the following complex normal form (Kuznetsov, 1998)

$$\dot{z} = \lambda(\mu) z + \sum_{2 \le k+l \le 3} \frac{1}{k!l!} g_{kl}(\mu) z^k \bar{z}^l + O\left(|z|^4\right). \tag{B.2}$$

Equation (B.2) can be transformed by a smooth and invertible parameter-dependent change of complex coordinate to (Kuznetsov, 1998)

$$\dot{w} = \lambda(\mu) w + c_1(\mu) w |w|^2 + O\left(|w|^4\right), \tag{B.3}$$

where

$$c_1(0) = \frac{\mathrm{j}}{2\omega_0}\left(g_{20}g_{11} - 2|g_{11}|^2 - \frac{1}{3}|g_{02}|^2\right) + \frac{g_{21}}{2}.$$

The Lyapunov coefficient c_1 has to be nonzero in order to satisfy the nondegeneracy condition. Then, the equation (B.3) can be transformed into the form of (B.1) by a parameter-dependent linear coordinate scaling, a time rescaling, and a nonlinear time reparametrization (Kuznetsov, 1998). We can thus derive

$$\mu_2 = \frac{-\Re(c_1(0))}{\alpha'(0)}.$$

We see that the sign of μ_2 determines the direction of the Hopf bifurcation. If $\mu_2 > 0$, the Hopf bifurcation is supercritical, whereas for $\mu_2 < 0$, the Hopf bifurcation is subcritical.

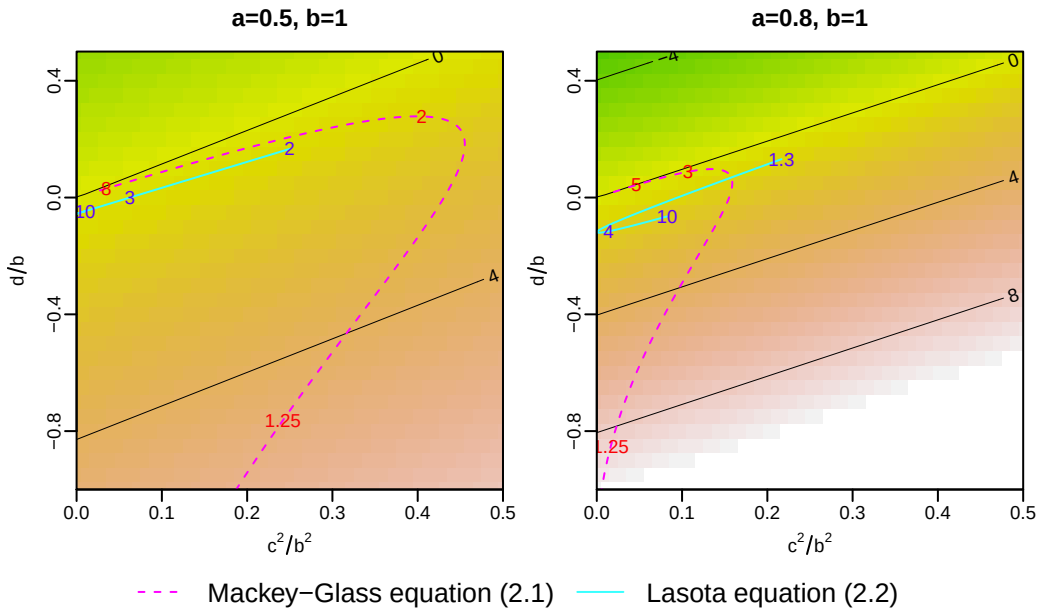

Figure B.1: Density plot of μ_2 with loci traced by the Mackey-Glass and Lasota equations as parameter x_* is varied. Higher values of μ_2 result in smaller limit cycles. The Mackey-Glass equation has higher μ_2 for smaller x_*but then approaches $\mu_2 = 0$ for larger x_*. μ_2 for the Lasota equation is less sensitive to variations in x_* and hence is more robust.

B.2 Calculation of μ_2 for systems with time-delayed nonlinearity

On considering the Taylor series expansion of (1.1) about an equilibrium point, we get

$$\dot{u}(t) = -a\,u(t) - b\,u(t-\tau) - c\,u(t-\tau)^2 - d\,u(t-\tau)^3 + O\left(u\,(t-\tau)^4\right). \quad \text{(B.4)}$$

See (Raina, 2005) and references therein to compute μ_2. Note that $\epsilon\,(\mu) = \sqrt{\mu/\mu_2}$ gives the amplitude of limit cycles for small μ.

We have

$$\mu_2 = \mu_{c^2}\,(c/b)^2 - \mu_d\,(d/b)\,, \quad \text{(B.5)}$$

where

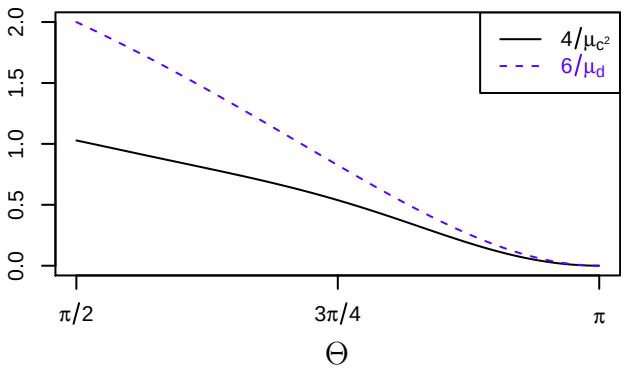

Figure B.2: A plot showing the coefficients of μ_2 (B.5). As $n \to 0$ in (2.2), we have an exponential production function $p(x) = \beta e^{-x}$. Without loss of generality, let $\gamma = 1$. Then, the Taylor series coefficients are $a = 1$, $b = \beta$, $c = -\beta/2$, and $d = \beta/6$. From (B.5), we get $\mu_2 = \mu_{c^2}/4 - \mu_d/6$. Since $\mu_{c^2}/4 > \mu_d/6$, Hopf bifurcation oscillations are always supercritical ($\mu_2 > 0$) for the equation $\dot{x}(t) = \beta e^{-x(t-\tau)} - x(t)$.

$$\mu_d = 3\frac{\Theta - \cos\Theta \sin\Theta}{\Theta \sin^2\Theta} = \frac{3}{1 - a^2/b^2}\left(1 + \frac{a/b}{b\tau_c}\right),$$

and

$$\begin{aligned}\mu_{c^2} &= \frac{6\Theta(10 - \cos 2\Theta + 6\cos\Theta) - 18\sin\Theta - 35\sin 2\Theta}{-7\sin 3\Theta + 9\sin 4\Theta - \sin 5\Theta - 2\sin 6\Theta} \Big/ 6\Theta(5+4\cos\Theta)\sin^2\Theta \sin^2\tfrac{\Theta}{2} \\ &= \frac{2\left(32a^5/b^5 - 8a^4/b^4 - 68a^3/b^3 - 2a^2/b^2(4 + 3b\tau_c) + a/b(59 - 18b\tau_c) - 3(2 - 11b\tau_c)\right)}{3b\tau_c(5 - 4a/b)(1 - a/b)(1 + a/b)^2}.\end{aligned}$$

Bibliography

1. **an der Heiden, U.** and **M. C. Mackey** (1982). The dynamics of production and destruction: analytic insight into complex behavior. *Journal of Mathematical Biology*, **16**(1), 75–101.

2. **Bélair, J.**, **L. Glass**, **U. a. d. Heiden**, and **J. Milton** (1995). Dynamical disease: identification, temporal aspects and treatment strategies of human illness. *Chaos: An Interdisciplinary Journal of Nonlinear Science*, **5**(1), 1–7.

3. **Beuter, A.** and **K. Vasilakos** (1995). Tremor: Is parkinson's disease a dynamical disease? *Chaos: An Interdisciplinary Journal of Nonlinear Science*, **5**(1), 35–42.

4. **Carr, J.** (2006). Center manifold. *Scholarpedia*, **1**(12), 1826.

5. **Echt, D. S.**, **P. R. Liebson**, **L. B. Mitchell**, **R. W. Peters**, **D. Obias-Manno**, **A. H. Barker**, **D. Arensberg**, **A. Baker**, **L. Friedman**, **H. L. Greene**, *et al.* (1991). Mortality and morbidity in patients receiving encainide, flecainide, or placebo. *New England Journal of Medicine*, **324**(12), 781–788.

6. **Glass, L.** and **M. C. Mackey**, *From clocks to chaos: The rhythms of life*. Princeton, NJ: Princeton University Press, 1988.

7. **Kuznetsov, Y. A.**, *Elements of applied bifurcation theory*, volume 112. Springer, 1998.

8. **Lasota, A.** (1977). Ergodic problems in biology. *Asterisque*, **50**, 239–250.

9. **Mackey, M. C.**, *Case Studies in Mathematical Modeling–Ecology, Physiology and Cell Biology*, chapter 8. Mathematical models of hematopoietic cell replication and control. New Jersey: Prentice-Hall, 1997, 151–182.

10. **Mackey, M. C.** and **L. Glass** (1977). Oscillation and chaos in physiological control systems. *Science*, **197**(4300), 287–289.

11. **Mackey, M. C.** and **J. G. Milton** (1987). Dynamical diseases. *Annals of the New York Academy of Sciences*, **504**(1), 16–32.

12. **Raina, G.** (2005). Local bifurcation analysis of some dual congestion control algorithms. *Automatic Control, IEEE Transactions on*, **50**(8), 1135–1146.

13. **Wolfram Research, I.**, MATHEMATICA. Wolfram Research, Inc., 2010, version 8.0 edition.